Article

pubs.acs.org/Biomac

Cross-Linking and Degradation of Step-Growth Hydrogels Formed by Thiol–Ene Photoclick Chemistry

Han Shih and Chien-Chi Lin*

Department of Biomedical Engineering, Purdue School of Engineering and Technology, Indiana University - Purdue University at Indianapolis, Indianapolis, Indiana 46202, United States

ABSTRACT: Thiol–ene photoclick hydrogels have been used for a variety of tissue engineering and controlled release applications. In this step-growth photopolymerization scheme, four-arm poly(ethylene glycol) norbornene (PEG4NB) was cross-linked with dithiol containing cross-linkers to form chemically cross-linked hydrogels. While the mechanism of thiol–ene gelation was well described in the literature, its network ideality and degradation behaviors are not well-characterized. Here, we compared the network cross-linking of thiol–ene hydrogels to Michael-type addition hydrogels and found thiol–ene hydrogels formed with faster gel points and higher degree of cross-linking. However, thiol–ene hydrogels still contained significant network nonideality, demonstrated by a high dependency of hydrogel swelling on macromer contents. In addition, the presence of ester bonds within the PEG-norbornene macromer rendered thiol–ene hydrogels hydrolytically degradable. Through validating model predictions with experimental results, we found that the hydrolytic degradation of thiol–ene hydrogels was not only governed by ester bond hydrolysis, but also affected by the degree of network cross-linking. In an attempt to manipulate network cross-linking and degradation of thiol–ene hydrogels, we incorporated peptide cross-linkers with different sequences and characterized the hydrolytic degradation of these PEG-peptide hydrogels. In addition, we incorporated a chymotrypsin-sensitive peptide as part of the cross-linkers to tune the mode of gel degradation from bulk degradation to surface erosion.

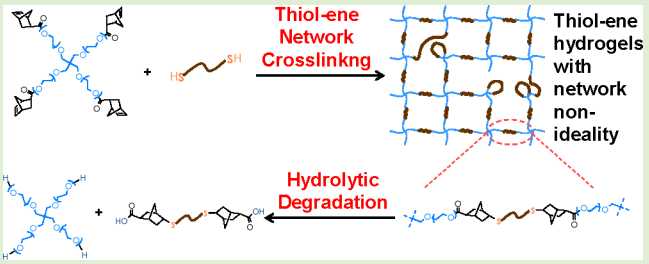

INTRODUCTION

An ongoing effort in biomaterial science and engineering is to design hydrogels with tunable and predictable degradation behaviors, because degradable hydrogels are particularly useful as provisional matrices for tissue regeneration and as carriers for controlled protein delivery.[1−4] Among all degradation mechanisms, hydrolytic degradation of synthetic hydrogels has received significant attention due to the simplicity of hydrolysis mechanism and well-defined polymer chemistry.[5−7] A classical way of preparing hydrolytically degradable hydrogels is by chain-growth photopolymerization of acrylated macromers, such as terminally acrylated poly(lactic acid)-*b*-poly(ethylene glycol)-*b*-poly(lactic acid) (acryl-PLA-*b*-PEG-*b*-PLA-acryl) triblock copolymers.[5,8] The hydrolytic degradation rate of these hydrogels could be tuned and predicted by using copolymers with different lengths of lactide repeating units.[6,7] Similarly, other hydrolytically labile ester bonds could be incorporated to the termini of PEG macromers prior to acrylation or methacrylation.[9,10]

In addition to the chain-growth polymerized hydrogels, step-growth polymerized gels could also be rendered hydrolytically degradable. For example, Hubbell and co-workers developed Michael-type addition hydrogels through nucleophilic reactions between acrylates on multiarm PEG macromer and sulfhydryl groups on the cross-linkers.[11,12] Thioether-ester linkages formed between acrylate and sulfhydryl moieties were hydrolytically labile and the degradation rates of these hydrogels could be tuned by controlling macromer concentration and functionality.[11,13,14] Bowman and colleagues performed experimental and theoretical investigations on hydrolytic degradation of step-growth thiol-acrylate and thiol-allylether photopolymers.[15−18] Degradation was readily tuned and predicted using monomers with different concentration, functionality, and degradability. More recently, Leach and colleagues developed hydrolytically degradable Michael-type hydrogels based on 4-arm PEG-vinylsulfone (PEGVS) and PEG-diester-dithiol.[19,20] Degradation of these step-growth hydrogels was altered by tuning the number of methylene groups between the thiol and ester moieties in the PEG-diester-dithiol linkers.

While these degradable hydrogels have found various successful applications, limitations and challenges exist. For instance, chain-growth photopolymerized hydrogels are known to form dense hydrophobic polyacrylate chains[21] that yield network heterogeneity and high molecular weight degradation products.[5−7] On the other hand, the formation of step-growth Michael-type hydrogels often requires long gelation time that leads to the formation of high degrees of network defects.[13] It has been shown that high macromer functionalities (e.g., 8-arm PEG-acrylate) and concentrations (e.g., >50 wt %) were

Received: January 8, 2012
Revised: June 17, 2012
Published: June 18, 2012

necessary for step-growth Michael-type addition hydrogels to approach an "ideal" network structure.[13]

To overcome the disadvantages facing hydrogels formed by chain-growth photopolymerizations and step-growth Michael-type addition reactions, Anseth and colleagues recently introduced a new class of PEG-peptide hydrogels based on a radical-mediated orthogonal thiol−ene photoclick reaction.[22] In this system, low intensity and long wavelength (5−10 mW/cm^2, 365 nm) ultraviolet light was used to generate thiyl radicals (from bis-cysteine-containing oligopeptides), which cross-linked with ene moieties on norbornene-functionalized 4-arm PEG (PEG4NB) to form a step-growth network. This reaction scheme preserves all advantages offered by photopolymerizations, including rapid, ambient, and aqueous reaction conditions, as well as spatial-temporal control over gelation kinetics. Step-growth thiol−ene photoclick reactions are not oxygen inhibited,[23] thus, yielding more rapid gelation kinetics compared to chain-growth photopolymerizations.[24] When compared to step-growth Michael-type gelation, thiol−ene photoclick reactions have reduced disulfide bond formation due to radical-mediated cleavage,[25] thus, increasing the extent of cross-linking that results in higher mechanical properties at similar macromer contents.[22] Furthermore, the orthogonal and step-growth nature of the norbornene-sulfhydryl reaction permits dynamic modification of hydrogel biochemical and biophysical properties in the presence of cells.[22] Several cell types have been encapsulated successfully by these PEG-peptide hydrogels, including human mesenchymal stem cells,[26] fibroblasts,[22,27] fibrosarcoma,[27] valvular insterstitial cells,[28] and radical-sensitive pancreatic β-cells.[24] Enzymatically degradable peptides could also be utilized to cross-link thiol−ene hydrogels for enzyme-responsive controlled release applications.[29]

While thiol−ene photopolymerized hydrogels have emerged as an attractive class of biomaterials, the structure−property relationships of these hydrogels have not been extensively characterized. For example, an "ideal network" was often mentioned in previous publications, even with the use of low macromer concentrations (2−10 wt % of PEG4NB) and no detailed characterization of hydrogel network properties was performed.[22,26,29] Furthermore, these thiol−ene hydrogels are susceptible to hydrolytic degradation due to the presence of an ester bond between the cyclic olefin and PEG backbone (Scheme 1). Here, we report the improved network cross-linking of thiol−ene hydrogels as compared to Michael-type addition hydrogels with similar macromer formulations. We also systematically study the hydrolytic degradation behaviors of thiol−ene hydrogels through experimental efforts and theoretical modeling. A statistical-co-kinetics model developed by Metters et al. for predicting hydrolytic degradation of step-growth Michael-type addition hydrogels was employed to predict the hydrolytic degradation of thiol−ene hydrogels due to their similarity in the degradation mechanism and the network structure.[13,30]

Scheme 1. Schematics of Photopolymerization and Hydrolytic Degradation of Step-Growth Thiol−Ene Hydrogels[a]

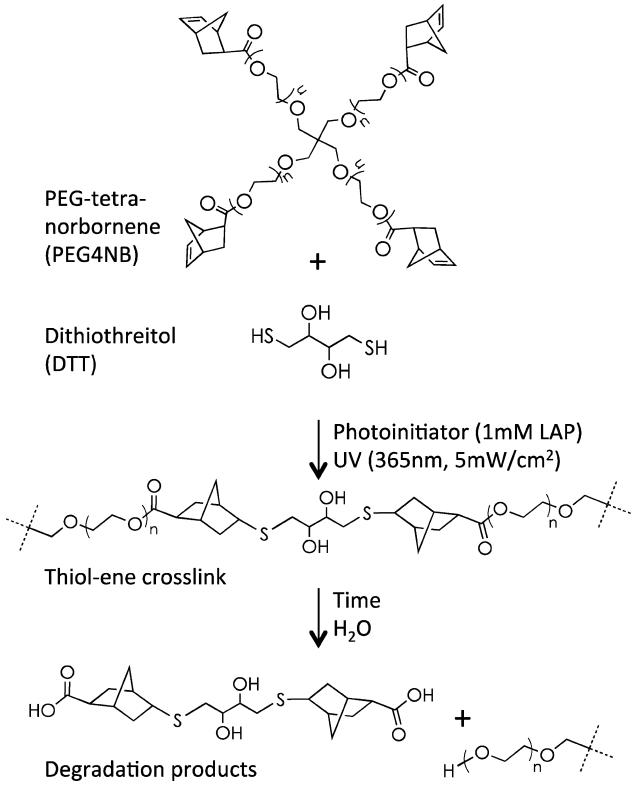

[a]PEG-tetra-norbornene (PEG4NB) reacts with a bi-functional cross-linker DTT (dithiothreitol), in a step-growth manner, to form thioether linkage and crosslinked hydrogels. Hydrolytic degradation of the network occurs due to ester bond hydrolysis.

EXPERIMENTAL SECTION

Materials. 4-Arm PEG−OH was purchased from JenKem Technology, U.S.A. Fmoc amino acids and coupling reagents for peptide synthesis were acquired from Anaspec. All other chemicals were obtained from Sigma-Aldrich unless noted otherwise.

Synthesis of PEG Macromers and Photoinitiator. Poly(ethylene glycol)-tetra-norbornene (PEG4NB) was synthesized using an established protocol.[22,26] Briefly, norbornene anhydride was formed by reacting 5-norbornene-2-carboxylic acid (5-fold excess of −OH group on multiarm PEG) and coupling reagent *N*,*N*′-dicyclohexylcarbodiimide (DCC, 2.5-fold excess of −OH group) in anhydrous dichloromethane (DCM) for 15 min at room temperature. The latter was filtered through a fritted funnel into a second flask containing 4-arm PEG−OH (20 kDa), 4-(dimethylamino)pyridine (DMAP, 0.5-fold of −OH group), and pyridine (5-fold excess of −OH group) in DCM (kept in an ice bath). After an overnight reaction, the product was washed with 5% sodium bicarbonate solution twice and brine once, followed by precipitation in cold ethyl ether. The product was then filtrated, redissolved in minimum amount of DCM, and reprecipitated in ether. Poly(ethylene glycol)-tetra-acrylate (PEG4A) was synthesized through reacting 4-arm PEG−OH (20 kDa) with acryloyl chloride (4-fold excess of −OH group) in the presence of triethylamine (TEA, 4.4-fold excess of −OH group) in toluene.[8,31] After an overnight reaction, the solution was filtered through a thin layer of neutral aluminum oxide. Sodium carbonate was added to the solution and the heterogeneous solution was stirred for 2 h in the dark. The solution was then filtered through Hyflo filtration aid and the clear solution obtained was precipitated in cold ether. High degree of PEG functionalization (>90%) was confirmed by ^{1}H NMR (Bruker 500). The synthesis of photoinitiator lithium arylphosphinate (LAP) was performed as reported elsewhere.[32]

Microwave-Assisted Solid-Phase Peptide Synthesis (SPPS). All peptides were synthesized and cleaved in a microwave peptide synthesizer (CEM Discover SPS) following standard solid phase peptide synthesis procedure using Fmoc-protected amino acids. Cleaved peptides were precipitated in cold ether, dried in vacuo, purified by reverse phase HPLC (PerkinElmer Flexar system), and characterized with mass spectrometry (Agilent Technologies). The purity of the synthesized peptides was at least 90%.

Hydrogel Fabrication and Swelling. Step-growth thiol−ene hydrogels were formed by radical-mediated photopolymerization between macromer PEG4NB and dithiol containing cross-linkers, such as dithiothreitol (DTT) or cysteine-containing peptides (Scheme 1). Unless otherwise stated, a unity molar ratio between thiol and ene groups was used (i.e., $R_{[thiol]/[ene]} = 1$). Thiol−ene photopolymerization was initiated by 1 mM LAP under ultraviolet light exposure (365 nm, 5 mW/cm^2) in double distilled water (ddH_2O) or aqueous buffered solutions for 3 min. Step-growth Michael-type addition hydrogels were formed between PEG4A and DTT at pH 8.0. Step-growth Michael-type hydrogels were formed from PEG4A and DTT (at stoichiometric ratio) in a humidified oven (37 °C) overnight to ensure complete gelation.

For swelling studies, each gel was prepared from 50 μL of precursor solution. After gelation, hydrogels were incubated in ddH_2O at 37 °C on an orbital shaker for 24 h to remove un-cross-linked (sol fraction) species. Gels were then dried and weighed to obtain dried polymer weights (W_{dry}). The dried polymers were then incubated in 5 mL of buffer solution (pH 6.0, pH 7.4 or pH 8.0 PBS) at 37 °C on an orbital shaker. At predetermined time intervals, hydrogels were removed from the medium, blotted the gel surface with Kimwipe tissue, and weighed to obtained swollen weights ($W_{swollen}$). Hydrogel mass swelling ratios (q) were defined as

$$q = \frac{W_{swollen}}{W_{dry}} \tag{1}$$

As described by Metters et al.,[6,7] the mass swelling ratio (q) of a hydrolytically degrading network increases exponentially as a function of degradation time:

$$q = q_0 e^{-k_{hyd}t} \tag{2}$$

Here, q_0 represents the initial mass swelling ratio before significant occurrence of degradation and k_{hyd} is the apparent pseudo first-order ester hydrolysis rate constant, which was obtained via exponential curve fitting to the experimental swelling data.

Rheometry. For rheometrical property measurements, hydrogel slabs were fabricated between two glass slides separated by 1 mm thick spacers. Circular gel discs (8 mm in diameter) were punched out from the gel slabs using a biopsy punch and placed in pH 7.4 PBS for 48 h. Strain sweep (0.1−20%) oscillatory rheometry was performed on a Bohlin CVO 100 digital rheometer. Shear moduli of the hydrogels were measured using a parallel plate geometry (8 mm) with a gap size of 800 μm. Tests were performed in the linear viscoelastic region (LVR). In situ gelation rheometry for thiol−ene hydrogels was conducted in a UV cure cell at room temperature. Briefly, the macromer solution was placed on a quartz plate in the UV cure cell, and irradiated with UV light (Omnicure S1000, 365 nm, 5 mW/cm^2) through a liquid light guide. In situ gelation rheometry for Michael-type hydrogels was measured at 37 °C using an 8 mm parallel plate geometry. Time sweep in situ rheometry was performed with 10% strain, 1 Hz frequency, 0.1 N normal force, and a gap size of 100 μm. Gel point (i.e., crossover time) was determined at the time when storage modulus (G') surpassed loss modulus (G'').

Network Structure of Step-Growth Hydrogels. A perfectly cross-linked (or "ideal") thiol−ene or Michael-type hydrogel network without defects can be estimated by means of hydrogel equilibrium swelling.[13] Considering the structural information of the step-growth hydrogels (i.e., macromer molecular weight and functionality), the average molecular weight between cross-links ($\overline{M_c}$) is defined as[13]

$$\overline{M_c} = 2\left(\frac{MW_A}{f_A} + \frac{MW_B}{f_B}\right) \tag{3}$$

Here, MW_A and MW_B represent the molecular weight of PEG4NB (or PEG4A) and cross-linker, respectively. f_A and f_B are the number of reactive functionalities for PEG4NB (or PEG4A) and cross-linker. With a known $\overline{M_c}$, the ideal network cross-linking density or density of elastically active chains (ν_c) and polymer volume fraction (ν_2) can be calculated based on the Flory−Rehner theory:[33,34]

$$\nu_c = \frac{V_1}{\overline{M_c}\,\overline{v_2}} = \frac{-[\ln(1-\nu_2) + \nu_2 + \chi_{12}\nu_2^2]}{\nu_2^{1/3} - \frac{2\nu_2}{f_A}} \tag{4}$$

Here, $\overline{v_2}$ is the specific volume of PEG (0.92 cm^3/g at 37 °C), V_1 is the molar volume of water (18 cm^3/mol), and χ_{12} is the Flory−Huggins interaction parameter for a PEG−H_2O system (0.45). After obtaining ν_2, the ideal hydrogel mass swelling ratio q can be obtained using the following equation:

$$\nu_2 = \frac{\overline{v_2}}{(q-1)\overline{v_1} + \overline{v_2}} \tag{5}$$

where $\overline{v_1}$ is the specific volume of water (1.006 cm^3/g at 37 °C).

Prediction of Hydrolytic Degradation of Thiol−Ene Hydrogels. A statistical-co-kinetic model established by Metters and Hubbell for predicting the hydrolytic degradation of step-growth hydrogels was used to predict the degradation of step-growth thiol−ene hydrogels. This model not only considers ester bond hydrolysis kinetics, but also takes into account the structural information of the hydrogels, such as the connectivity of the ideal networks. Based on this model, the degradation of thiol−ene hydrogels was assumed to be purely due to ester bond hydrolysis with a pseudo-first-order degradation kinetics.[6,7] With this assumption, the fraction of hydrolyzed ester bonds (P_{ester}) at any given time in the system is expressed as

$$P_{ester} = 1 - \frac{[ester]}{[ester]_0} = 1 - e^{-k't} \tag{6}$$

Here, k' is the pseudo-first-order ester bond hydrolysis rate constant. The values for $[ester]$ and $[ester]_0$ are the current and initial number of intact ester bonds in the system.

The fraction of intact elastic chains (i.e., cross-linkers such as DTT or bis-cysteine containing peptides) within these cross-linked networks at any given time is expressed as

$$1 - P_{chain} = (1 - P_{ester})^N = e^{-Nk't} \tag{7}$$

where N is the number of degradable units (i.e., ester bonds) connected to one elastic chain (e.g., $N = 2$ in the case of PEG4NB-DTT hydrogels).

To obtain the degree of cross-linking in the system, one must also consider the connectivity of multiarm PEG macromers. For an ideal step-growth network, the fraction of f_A-arm macromer with i arms still connected to the network at any time point during ester hydrolysis is expressed as:[13]

$$F_{i,f_A} = \frac{f_A!}{(f_A - i)!\,i!} P_{chain}^{(f_A - i)}(1 - P_{chain})^i \tag{8}$$

With this information, the cross-linking density of the degrading network is expressed as

$$\nu_c = \left(\sum_{f_A}^{i=3} \frac{i}{2} F_{i,f_A}\right)[A]_0 \tag{9}$$

Here, $i \geq 3$ because any f_A-arm ($f_A \geq 3$) macromer with only two arms connected to intact elastic chains forms an extended loop rather than a cross-link. $[A]_0$ represents the concentration of f_A-arm macromers (e.g., PEG4NB) in the equilibrium swelling state before the onset of network degradation, which is correlated to the cross-linking density of a network:

$$\nu_{c,0} = \frac{f_A}{f_B}[A]_0 \tag{10}$$

When the functionalities of the macromer and cross-linker ($f_A = 4$ and $f_B = 2$) are taken into account, the cross-linking density of a perfectly cross-linked thiol−ene network in the equilibrium state could be derived from eqs 4−10 and expressed as

$$\nu_c = (6e^{-3Nk't} - 4e^{-4Nk't})[A]_{0,actual} \tag{11}$$

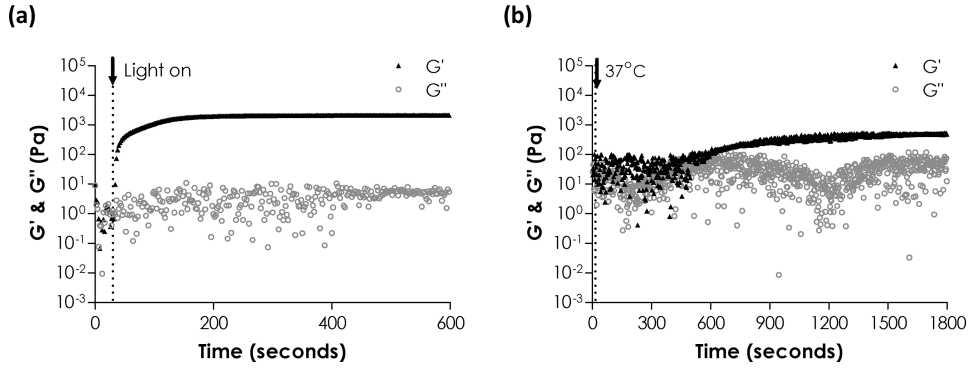

Figure 1. In situ rheometry of step-growth hydrogels: (a) Thiol−ene photoclick polymerization (4 wt % PEG4NB-DTT). UV light was turned on at 30 s. (b) Michael-type addition (4 wt % PEG4A-DTT). Temperature reached 37 °C at 15 s.

For gels with nonidealities, based on eqs 4, 5, and 11, $[A]_{0,\text{actual}}$ is obtained using actual cross-linking density:

$$[A]_{0,\text{actual}} = \frac{\nu_{c,\text{actual}}}{\nu_{c,\text{ideal}}}[A]_0 \tag{12}$$

where $\nu_{c,\text{actual}}$ represents the experimental cross-linking density converted from an experimental mass swelling ratio using eqs 4 and 5 and $\nu_{c,\text{ideal}}$ represents ideal cross-linking density calculated based on $\overline{M_c}$ derived from eq 3.

Enzymatic Degradation Study. The 4 wt % PEG4NB hydrogels (30 μL/gel) were cross-linked by bis-cysteine containing peptides with different percentages of chymotrypsin-sensitive (CGGY↓C: arrow indicates cleavage site) and nonsensitive (CGGGC) sequences. Hydrogels were fabricated using methodology described above and incubated in 500 μL of PBS containing 0.5 mg/mL of chymotrypsin (Worthington Biochemical) at room temperature on an orbital shaker. At specific time points, hydrogels were removed from the chymotrypsin solution, blotted dry, the swollen mass was measured, and then the hydrogel was placed back into the chymotrypsin solution. Fresh chymotrypsin solution was prepared every 15 min to ensure enzyme activity. Percent mass loss is defined as

$$\text{Mass loss}(\%) = \frac{W_t - W_0}{W_0} \times 100\% \tag{13}$$

where W_t is the gel weight measured at specific time points and W_0 is the mass measured at equilibrium swelling (48 h).

Data Analysis. Data analysis and curve fitting were performed on Prism 5 software. The pseudo-first-order rate constant (k') was determined using Matlab 2010 built-in curve-fit tool function. A best-fit k' was determined based on Matlab built-in trust region algorithm with an R^2 value of 0.95 or greater. Unless otherwise noted, all experiments were conducted independently three times, and the results were reported as mean ± SD.

RESULTS AND DISCUSSION

Network Cross-Linking of Thiol−Ene and Michael-Type Hydrogels. The network ideality and hydrolytic degradation behaviors of step-growth thiol−ene hydrogels received little attention in previous reports. Given the attractive features offered by this new class of biomaterials, we were interested in characterizing and understanding these properties. In addition, while it has been suggested that thiol−ene photopolymerization produces hydrogels with higher degree of cross-linking when compared to Michael-type addition hydrogels, no direct experimental comparison has been made to verify this claim. Here, we prepared step-growth thiol−ene or Michael-type hydrogels using PEG4NB or PEG4A macromers. DTT was used as a hydrogel cross-linker for both systems. Because PEG4NB and PEG4A used in this study have the same molecular weight (MW_A = 20 kDa) and functionality (f_A = 4), hydrogels cross-linked by these macromers without any structural defect would have the same degree of cross-linking at identical macromer concentration. Therefore, variations in hydrogel physical properties (e.g., swelling, modulus, etc.) could be used to evaluate the network connectivity. We first characterized the gelation kinetics of these two step-growth hydrogel systems via in situ rheometry. As shown in Figure 1, the gel point of the thiol−ene photoclick reaction was ∼230-fold faster than that of the Michael-type addition reaction (3 ± 1 vs 689 ± 18 s). While the time required to reach complete gelation for thiol−ene photoclick reaction was less than 3 min (Figure 1a), it took almost 25−30 min for the Michael-type reaction to reach complete gelation (Figure 1b). In addition, the final shear modulus (G') for thiol−ene hydrogels was 4.3-fold higher than that of Michael-type hydrogels (2030 ± 80 vs 470 ± 20 Pa), indicating improved network connectivity in thiol−ene hydrogels.[1,35,36]

We further compared these two gel systems using hydrogel equilibrium swelling and shear modulus, both of which are directly related to the hydrogel cross-linking density.[36] Based on eq 3, the molecular weight between cross-links ($\overline{M_c}$) of these two step-growth hydrogel systems without defect should be identical (neglecting the minor difference in the molecular weight of norbornene and acrylate moiety) and was calculated as 10154 Da. Accordingly, the mass swelling ratio of a perfectly cross-linked step-growth hydrogel ($q_{\text{eq,ideal}}$) was calculated as 9.6 using eqs 4 and 5 (Table 1 and dashed line in Figure 2).

Table 1. Characteristics of Step-Growth Michael-Type and Thiol−Ene Hydrogels (4 wt %, 20 kDa, 4-Arm PEG-Derivatives Cross-Linked by DTT, pH 7.4, N = 4)

	$\overline{M_c}$ (g/mol)	$q_{\text{eq,ideal}}$	$q_{\text{eq,actual}}$	$G'_{\text{eq,actual}}$ (kPa)
PEG4A (Michael-type)	10154	9.6	44.5 ± 3.8	0.2 ± 0.01
PEG4NB (thiol−ene)	10154	9.6	28.5 ± 2.2	1.1 ± 0.1

Experimentally, however, we found that thiol−ene hydrogels, when compared to Michael-type gels at identical macromer compositions, had a lower mass swelling ratio (28.5 ± 2.2 vs 44.5 ± 3.8) and higher elastic modulus (∼1 vs ∼0.2 kPa) at the equilibrium state. These experimental results confirmed a previous notion that the radical-mediated thiol−ene reaction, when compared to the Michael-type conjugation reaction, produce step-growth hydrogels with faster gelation kinetics, less

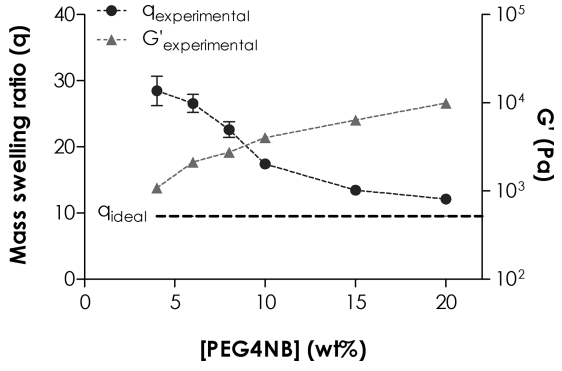

Figure 2. Effect of PEG4NB macromer concentration on hydrogel equilibrium swelling (left *y*-axis) and elastic modulus (right *y*-axis). Swelling ratio of an ideal network was calculated based on the molecular weight between cross-links ($\overline{M_c}$) of given macromer molecular weights (MW_{PEG4NB} = 20 kDa, MW_{DTT} = 154 Da) and functionalities (f_{PEG4NB} = 4, f_{DTT} = 2).

structural defects, higher degree of cross-linking, and improved gel mechanical properties.[22]

Effect of Macromer Concentrations on Thiol−Ene Hydrogel Network Cross-Linking. As shown in Table 1, an "ideal" step-growth network with a fixed macromer composition and without defect should only have a single equilibrium swelling ratio. Furthermore, the swelling ratio should be independent of macromer concentrations at equilibrium state. The experimental equilibrium mass swelling ratios of PEG4NB-DTT gels, however, exhibited high dependency on PEG4NB macromer concentration, as shown in Figure 2. For example, when the concentration of PEG4NB macromer was increased from 4 to 20 wt %, swelling ratios decreased from 28.5 ± 2.2 to 12.1 ± 0.2 and approached ideal equilibrium swelling ratio (9.6). Hydrogels with low swelling ratios (at higher macromer contents) had higher elastic moduli (~1 and ~10 kPa for 4 and 10 wt % PEG4NB-DTT hydrogels, respectively). This inverse relationship was commonly observed in chemically cross-linked networks, including chain-growth PEGDA hydrogels.

The trend observed in Figure 2 could be attributed to a higher tendency of cyclization at lower PEG4NB contents. At diluted macromer concentrations, a higher extent of intramolecular reactions led to formation of more primary cycles. Consequently, a lower degree of intermolecular cross-linking resulted in increased gel swelling and vice versa.[13] The network defects resulting from different degrees of intramolecular and intermolecular reactions were the major reason for the dependency of experimental equilibrium swelling ratios on macromer concentrations.[13]

The strong dependency between macromer concentration (especially at lower concentrations) and network ideality in thiol−ene hydrogels was beneficial in that the physical properties (e.g., swelling and modulus) of these thiol−ene hydrogels could be easily tuned for biological applications (Figure 2). For example, hydrogel shear moduli obtained (~1 to 10 kPa) using current thiol−ene hydrogel formulations were within a physiologically relevant range and could be used to study the effect of matrix stiffness on cell fate processes.[37,38] More importantly, the gelation time for these thiol−ene hydrogels was drastically shortened when compared to the cross-linking of chain-growth PEGDA or step-growth Michael-type hydrogels.

Effect of pH on Degradation of PEG4NB-DTT Hydrogels. As stated previously, thiol−ene hydrogels could be degraded hydrolytically via ester hydrolysis. We found thiol−ene hydrogels degradation to be pH-dependent (Figure 3).

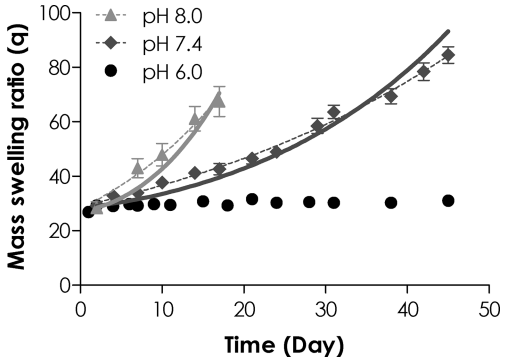

Figure 3. Effect of buffer pH on mass swelling ratio of 4 wt % PEG4NB-DTT hydrogels. Symbols represent experimental data while dashed curves represent exponential curve fitting to the experimental data. The apparent degradation rate constants (k_{hyd}) for gels degraded in pH 7.4 and pH 8.0 were 0.024 ± 0.001 and 0.057 ± 0.002 day^{-1}, respectively. Solid curves represent model predictions with best-fit kinetic rate constants: $k'_{pH7.4}$ = 0.011 day^{-1} and $k'_{pH8.0}$ = 0.027 day^{-1}. No curve fitting or model prediction was made for gels degraded in pH 6.0 due to the stability of gels in acidic conditions.

PEG4NB-DTT hydrogels incubated in acidic conditions (pH 6.0) were stable with an almost constant swelling ratio over a 45-day period, whereas hydrogels with the same compositions exhibited increasing swelling over time in slightly basic conditions (pH 7.4 and pH 8.0). We conducted exponential curve fittings using the swelling data of degrading hydrogels and found high degree of correlation between the fitted curves with the experimental data (dashed curves, R^2 = 0.98 for both pH 7.4 and 8.0 in Figure 3), indicating that the degradation of thiol−ene hydrogels was most likely a result of pseudo-first order ester bond hydrolysis.

Because the two basic pH conditions yielded significantly different degradation rates (Table 2), we were interested to know if gel degradation in different pH values assumed the same degradation mechanism. A previous study concerning the degradation of thiol−acrylate photopolymer networks revealed that, if the degradation follows the same ester hydrolysis mechanism at an elevated pH value (e.g., from pH 7.4 to pH 8.0), the two degradation profiles could be described using a pseudo-first-order equation:[17]

$$[\text{ester}] = [\text{ester}]_0 e^{-k'[\text{OH}^-]t} \quad (14)$$

In the above equation, the influence of hydroxyl ion concentration was separated from the pseudo-first-order kinetic constant, because pH was no longer a constant in the experimental setting. If the network degradation was purely due to ester bond hydrolysis in different pH values, the degradation could still be described using the same ester hydrolysis rate constant (k') if a factor of 4 was multiplied to the degradation time. In another word, the two degradation curves (at pH 7.4 and 8.0) would overlap after adjusting the degradation time to account for the 4-fold increase in the OH^- ion concentrations between the two pH values.[17] Similarly, the factor of 4 could be incorporated into k' to reflect the accelerated degradation kinetics. Consequently, one would

dx.doi.org/10.1021/bm300752j | Biomacromolecules 2012, 13, 2003−2012

Table 2. Hydrolytic Degradation Rate Constants for PEG4NB-DTT Hydrogel Network[a]

[PEG4NB] (wt%)	pH	k_{hyd} (day^{-1})	R^2_{khyd}	ratio of $k_{hyd,pH8.0}/k_{hyd,pH7.4}$	k' (day^{-1})	$R^2_{k'}$	ratio of $k'_{pH8.0}/k'_{pH7.4}$
4	7.4	0.024 ± 0.001	0.98	2.4	0.011	0.96	2.5
	8.0	0.057 ± 0.002	0.98		0.027	0.98	
10	7.4	0.020 ± 0.001	0.98	2.5	0.009	0.95	2.3
	8.0	0.050 ± 0.001	0.99		0.021	0.96	

[a]The k_{hyd} and k' values were obtained from exponential fit and statistical-co-kinetic model fit, respectively, to the swelling data (pH 7.4, N = 4).

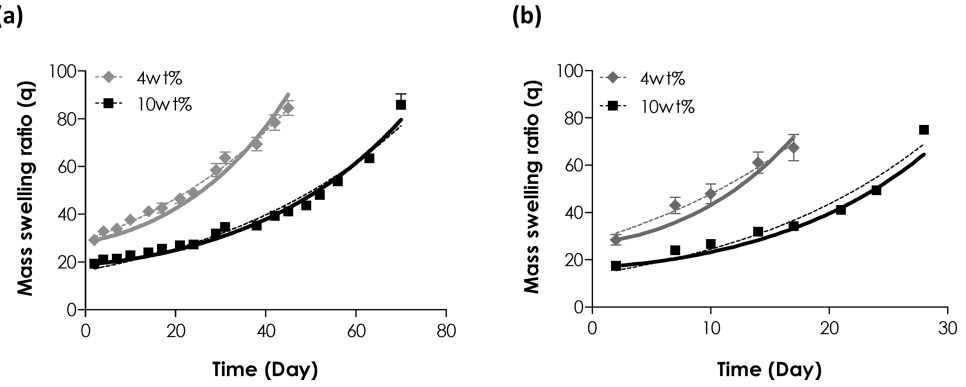

Figure 4. Hydrolytic degradation of PEG4NB-DTT hydrogels with different macromer concentrations in (a) pH 7.4 and (b) pH 8.0 PBS. Symbols represent experimental data, dashed curves represent exponential fit, and solid curves represent model prediction (see Table 2 for hydrolysis rate constants selected).

expect to obtain a 4-fold increase in the ratio of the apparent degradation rate constants (k_{hyd}) for hydrogels degraded in the two pH values. However, the exponential curve fitting performed in Figure 3 (k_{hyd} = 0.057 ± 0.002 and 0.024 ± 0.001 day^{-1} pH 8.0 and 7.4, respectively) yielded a k_{hyd} ratio of 2.4, rather than the ideal 4-fold increase (Table 2). This significantly lowered k_{hyd} ratio suggested that the degradation was not solely governed by simple ester bond hydrolysis and other factors could also play a role on the degradation rate of these thiol−ene hydrogels.

In addition to the experimental work, we also utilized a statistical-co-kinetic model to predict the hydrolytic degradation of thiol−ene hydrogels. Using this model (eq 11), we chose a best-fit k' of 0.011 day^{-1} (R^2 = 0.96) and 0.027 day^{-1} (R^2 = 0.95) for the degradation of 4 wt % PEG4NB-DTT hydrogels in pH 7.4 and 8.0, respectively (Table 2). Note that these k' values were selected only to validate the model predictions at different degradation conditions and by no means to suggest any "ideality" in the cross-linked network because the gels at these conditions were not "ideal", as discussed in the previous sections. As stated above, if the thiol−ene network degradation was governed solely by ester bond hydrolysis, a k' of 0.044 day^{-1} (4-fold of $k'_{pH7.4}$ = 0.011 day^{-1}) could be used to predict gel degradation occurred at pH 8.0. However, the best-fit k' was 0.027 day^{-1} (R^2 = 0.95) for degradation occurred at pH 8.0 that only yielded a ratio of 2.5 (compared to $k'_{pH7.4}$ = 0.011 day^{-1}) and, again, was much slower than the theoretical 4-fold difference (Table 2). A potential explanation for this phenomenon is base-catalyzed oxidation of thioether bond forming between norbornene and thiol groups (Scheme 1), which was likely promoted at higher pH values[39] and influenced the rate of ester hydrolysis. Another possible reason for the lower-than-predicted degradation rate at higher pH values was that the degradation process produced acidic byproduct (Scheme 1), which decreased acidity and retarded the degradation. Further investigations, however, are required to elucidate the exact mechanisms.

Effect of Macromer Concentration on Degradation of PEG4NB-DTT Hydrogels. We further evaluated the hydrolytic degradation of PEG4NB-DTT hydrogels with different macromer concentrations (4 and 10 wt %) in pH 7.4 (Figure 4a) and pH 8.0 (Figure 4b). We observed experimentally that hydrogels prepared from a precursor solution containing lower weight content of PEG4NB (e.g., 4 wt %) degraded at a slightly faster rate (e.g., 0.024 ± 0.001 and 0.020 ± 0.001 day^{-1} for 4 and 10 wt % PEG4NB at pH 7.4, respectively; Table 2), regardless of pH value. Model prediction also followed the same trend where higher best-fit k' values were obtained for gels made from lower PEG4NB concentration (e.g., 0.011 and 0.009 day^{-1} for 4 and 10 wt % PEG4NB at pH 7.4, respectively; Table 2). This study suggested that the effect of macromer concentration affected not only the initial network cross-linking (i.e., network ideality) but also the rate of network hydrolytic degradation.

Effect of Initial Cross-Linking Density on Degradation of PEG4NB-DTT Hydrogels. Results in Figure 4 revealed that the degradation rate of thiol−ene hydrogels could be affected by the degree of initial network cross-linking, a characteristic different from Michael-type addition hydrogels. To further validate this observation, we conducted additional studies using both theoretical and experimental approaches. We first predicted, using eq 11, the degradation profiles of ideal thiol−ene hydrogels with different degrees of cross-linking by varying the stoichiometric ratios of thiol to ene moieties (i.e., $R_{[thiol]/[ene]}$ = 0.6, 0.8, and 1). This parametric manipulation yielded hydrogels with different initial cross-linking densities ($[A]_{0,ideal}$ = 5.78 × 10^{-4}, 7.71 × 10^{-4}, and 9.63 × 10^{-4} M for $R_{[thiol]/[ene]}$ = 0.6, 0.8, and 1, respectively). In these predictions, a fixed hydrolysis rate constant (k' = 0.063 day^{-1}) was selected based on a value reported for the degradation of step-growth Michael-type hydrogels.[30] As shown in Figure 5, the ideal initial mass swelling ratio at different degree of network cross-linking ($R_{[thiol]/[ene]}$ = 0.6, 0.8, and 1) varied only slightly between 9.6 and 11.9. Because the assumption in this prediction was that the rate of degradation is independent of the initial degree of

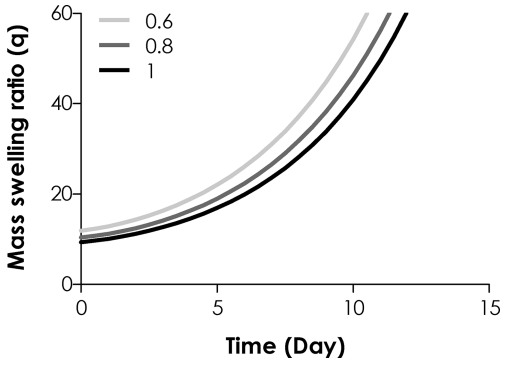

Figure 5. Model prediction of thiol−ene hydrogel degradation starting from different initial cross-linking ($R_{[thiol]/[ene]}$ = 0.6, 0.8, and 1; k' = 0.063 day^{-1}).

network cross-linking, a single k' yielded three degradation profiles with only slight variation.

To validate the prediction shown in Figure 5, we designed thiol−ene hydrogels with different initial degree of cross-linking by altering the concentrations of cross-linker used (DTT, $R_{[thiol]/[ene]}$ = 0.6, 0.8, and 1) while keeping a constant PEG4NB macromer content (4 wt %) during gelation. As expected, decreasing initial network cross-linking (e.g., $R_{[thiol]/[ene]}$ = 0.6) resulted in a significant increase in initial hydrogel swelling (q = 69.2 ± 3.0) due to increased network nonideality (Figure 6a). This phenomenon was similar to the results shown in Figure 2 where hydrogels prepared from lower PEG4NB weight contents had significantly higher initial swelling. When the difference in the initial degree of swelling was taken into account in the model prediction, one would expect similar degradation trends as shown in Figure 5 where the profiles could be predicted using a single k'. Interestingly, our experimental results showed that thiol−ene network cross-linked with low $R_{[thiol]/[ene]}$ exhibited not only very high equilibrium swelling ratios, but also much faster degradation rates (Table 3). When the degradation profiles were fitted with eq 11, the best-fit k' values were 0.035, 0.017, and 0.011 day^{-1} for $R_{[thiol]/[ene]}$ = 0.6, 0.8, and 1, respectively (Table 3). In another words, the degradation rate constants were accelerated (2- to 3-fold) as a function of network nonideality. The accelerated gel degradation was confirmed via rheometrical measurements where gels reached complete disintegration by day 21 and day 28 for $R_{[thiol]/[ene]}$ = 0.6 and 0.8, respectively (Figure 6b).

Table 3. Hydrolytic Degradation Rate Constants for PEG4NB-DTT Hydrogel Network with Different Stoichiometric Ratios[a]

$R_{[thiol]/[ene]}$	$[A]_{0,ideal}$ (M)	k_{hyd} (day^{-1})	R^2_{khyd}	k' (day^{-1})	$R^2_{k'}$
0.6	5.78×10^{-4}	0.073 ± 0.002	0.96	0.035	0.95
0.8	7.71×10^{-4}	0.035 ± 0.004	0.97	0.017	0.96
1	9.63×10^{-4}	0.024 ± 0.001	0.98	0.011	0.96

[a]The k_{hyd} and k' values were obtained from exponential fit and statistical-co-kinetic model fit, respectively, to the swelling data.

Results shown in Figures 4 and 6 were different from previous reports for hydrolytic degradation of Michael-type hydrogels. For example, the prediction and verification results from Metters et al. showed that a single k' could be used to describe the degradation occurred at different initial cross-linking densities, indicating the hydrolysis of thioether-ester bonds forming between PEG-acrylate and DTT was not affected by factors other than simple hydrolysis (e.g., macromer concentration, cross-linking efficiency, etc.).[13] In fact, previous models developed for predicting the hydrolysis of PEG hydrogels were based on the assumptions that the factors affecting hydrolysis could be "lumped" into a pseudo-first-order hydrolysis rate constant or k'.[5−7,13] These factors include water or hydronium ion concentrations, temperature, pH values, and so on. For highly swollen hydrogels (q > 10), these factors are often negligible at constant temperature and pH value, thus, the degradation profiles of the hydrogels could be predicted using the same k', regardless of macromer composition or degree of network cross-linking. While the degradation of thiol−ene hydrogels was mediated by ester bond hydrolysis, our data suggested that it was also affected by other environmental and structural factors (such as the presence of norbornane groups connecting the thioether and ester bonds). In addition, we found that the degradation of thiol−ene hydrogels was slower than the reported degradation of thiol−acrylate Michael-addition hydrogels at comparable macromer concentrations. We reason that this was due to the hydrophobic norbornane group connecting the thioether and ester bonds. In thiol−acrylate Michael-addition hydrogels, this linkage is a less hydrophobic ethylene group. The mechanisms or factors affecting the hydrolytic degradation rate of thiol−ene hydrogels at different initial cross-linking densities are yet to be determined. Nonetheless, a general trend observed from our studies was that thiol−ene hydrogels with a higher degree of

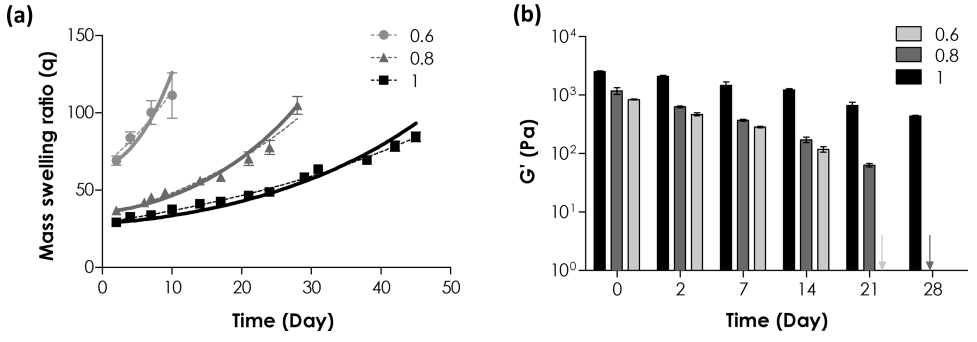

Figure 6. Effect of initial network cross-linking on PEG4NB-DTT hydrolytic degradation. (a) Mass swelling ratio and (b) elastic moduli of 4 wt % PEG4NB-DTT hydrogels with $R_{[thiol]/[ene]}$ = 0.6, 0.8, and 1. Symbols represent experimental data, dashed curves represent exponential fit, and solid curves represent model prediction (see Table 3 for degradation rate constants selected).

Table 4. Parameters for PEG4NB−Peptide Hydrogel Network[a]

peptide cross-linker	MW_B (Da)	gel point (s)	k_{hyd} (day^{-1})	R^2_{khyd}	k' (day^{-1})	$R^2_{k'}$
CGGGC	394	5.3 ± 0.1	0.049 ± 0.001	0.98	0.026	0.96
CGGYC	501	4.5 ± 0.5	0.036 ± 0.004	0.99	0.018	0.98
CGGLC	451	4.3 ± 1.4	0.036 ± 0.002	0.99	0.017	0.98

[a]The k_{hyd} and k' values were obtained from exponential fit and statistical-co-kinetic model fit, respectively, to the swelling data. (pH 7.4, N = 4).

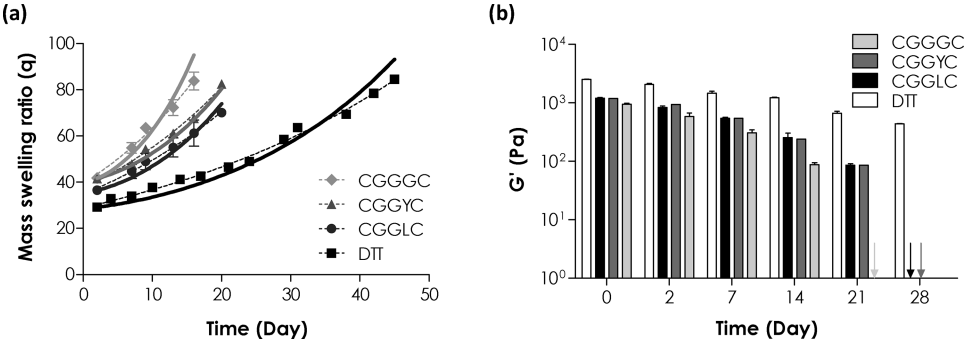

Figure 7. Effect of cross-linker peptide sequences on PEG4NB−peptide hydrogels degradation. (a) Mass swelling ratio and (b) elastic modulus of PEG4NB hydrogels cross-linked by CGGGC, CGGYC, or CGGLC peptides. PEG4NB-DTT hydrogels were used for comparison. Symbols represent experimental data, dashed curves represent exponential curve fits, and solid curves represent statistical-co-kinetics model fits to the experimental data (4 wt % PEG4NB−peptide hydrogels, pH 7.4, N = 4).

cross-linking degraded at a slower rate than gels with a lower degree of cross-linking.

Effect of Cross-Linker Sequence on Network Properties of PEG4NB−Peptide Hydrogels. In previous sections, we have learned that there was a high interdependency between the degree of thiol−ene hydrogel network cross-linking and the subsequent degradation rates using DTT as a hydrogel cross-linker. Recent studies have shown that PEG hydrogels cross-linked by peptide cross-linkers are useful in creating biomimetic extracellular microenvironments.[12,26] Here, we investigated the influence of peptide sequences on the cross-linking and degradation of step-growth thiol−ene hydrogels. As a model system to illustrate the importance of peptide sequences on thiol−ene hydrogel degradation, we synthesized three simple peptide cross-linkers with only one amino acid variation: CGGGC, CGGYC, and CGGLC. The molecular weights of these three peptide cross-linkers (MW_B) varied slightly between 394 to 501 Da (Table 4), which would only cause minimum influence in the chain length between adjacent cross-links due to the relatively large PEG4NB macromolecules (MW_A = 20 kDa) used.

Table 4 shows the physical properties of 4 wt % PEG4NB−peptide hydrogels cross-linked by peptide cross-linker with different sequences. These PEG4NB−peptide hydrogels all had rapid gel points (∼4−5 s), which were consistent with our previous studies in thiol−ene hydrogels.[24] Similar to the degradation of PEG4NB-DTT gels shown in Figures 4 and 6, PEG−peptide hydrogel degradation rates were affected by the initial degree of network cross-linking. As shown in Figure 7, peptide sequences affected both initial cross-linking as well as subsequent hydrolytic degradation rate. At the same macromer weight content (4 wt %), the initial swelling ratios of PEG4NB−peptide hydrogels were significantly higher than that of PEG4NB-DTT hydrogels. As a result, these PEG4NB−peptide hydrogels exhibited faster hydrolytic degradation rates (Table 4). Interestingly, hydrogels cross-linked by CGGGC and CGGYC peptides had similar initial swelling (Figure 7a), but the degradation rate constant was significantly lower for gels cross-linked by CGGYC (∼26% lower in k_{hyd}; ∼30% lower in k'; Table 4). Furthermore, hydrogels cross-linked by peptides containing aromatic (e.g., CGGYC) or hydrophobic (e.g., CGGLC) residues yielded slower degradation rates compared to gels cross-linked by simple CGGGC linker, potentially due to steric hindrance and hydrophobic effect of tyrosine and leucine residues that retarded degradation (Table 4). As expected, the swelling of these PEG4NB−peptide hydrogels was inversely correlated to the elastic moduli (Figure 7b). Hydrogels cross-linked by CGGGC peptide degraded completely in about 15 days (modulus dropped from ∼1.0 to ∼0.1 kPa from day 0 to day 14), while gels cross-linked with CGGYC or CGGLC lasted at least 21 days until complete gel disintegration. This study revealed that the degradation of thiol−ene hydrogels could be easily tuned by altering identity of the peptide cross-linkers.

Effect of Protease Sensitivity on Thiol−Ene Hydrogel Degradation. Many step-growth hydrogels have been prepared for protease-sensitive degradation by incorporating peptidyl substrates as hydrogel cross-linkers.[12,24,26,29,40−44] Here, we sought to combine enzymatic and hydrolytic degradation properties of thiol−ene hydrogels and create dual-mode degradable hydrogels without altering hydrogel molecular structure or hydrophilicity. By combining peptide cross-linkers with different protease sensitivities, we found that the degradation behaviors of thiol−ene hydrogels could be easily manipulated and changed from completely surface erosion to bulk degradation. Here, hydrogels were cross-linked by 4 wt % PEG4NB and stoichiometric ratio of non-cleavable CGGGC and chymotrypsin cleavable CGGY↓C peptides at various compositions (percent molar ratio of CGGYC/CGGGC = 100:0, 75:25, 50:50, 25:75, and 0:100, Figure 8). Note that the overall molar ratio of thiol to ene moieties was stoichiometric balanced for all conditions ($R_{[ene]/[thiol]}$ = 1). When these gels were exposed to chymotrypsin solution, hydrogels containing high percentage of CGGYC cross-linker (100−75%) eroded rapidly by surface erosion, evidenced by linearly increasing mass loss profiles with time. These gels

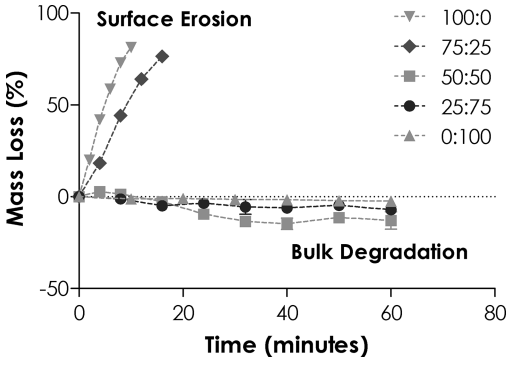

Figure 8. Effect of peptide cross-linkers on PEG4NB–peptide hydrogels erosion/degradation. PEG4NB hydrogels cross-linked by different percentage of chymotrypsin sensitive (CGGYC) and nondegradable (CGGGC) peptides. Figure legends indicate the percent molar ratio of CGGYC/CGGGC (4 wt % PEG4NB–peptide hydrogels, pH 7.4, $N = 4$).

reached complete erosion at around 10 and 16 min for gels incorporated with 100 and 75% of CGGYC, respectively (Figure 8). Interestingly, when the total content of CGGYC peptide was decreased to 50 and 25%, chymotrypsin treatment led to increased gel mass (i.e., negative mass loss). These gels continued to swell and gained mass for the remaining course of study, indicating that protease treatment led to a "loosened" gel structure and increased water uptake. The degradation mode was likely transitioned from a surface erosion to a bulk degradation mechanism. On the other hand, chymotrypsin treatment had no effect on the swelling or mass loss of thiol–ene hydrogels cross-linked by non-chymotrypsin sensitive linker (CGGGC). These results suggested that by altering protease sensitivity of PEG4NB–peptide hydrogels through elegant selection of peptide cross-linkers, the mode of degradation profiles could also be manipulated and may be used to dynamically control growth factor delivery in the future.

CONCLUSIONS

In summary, we showed that PEG hydrogels formed by step-growth thiol–ene photopolymerizations exhibited high degree of tunability in network cross-linking and degradation. In addition to the improved network properties compared to Michael-type hydrogels, we also found that thiol–ene hydrogels were hydrolytically degradable and the degradation was base-catalyzed and followed a bulk degradation mechanism. Through experimental and theoretical investigations, we found that the degradation of thiol–ene hydrogels was primarily governed by ester bond hydrolysis and was accelerated as network nonideality increases. In addition, we were able to tune and predict the hydrolytic degradation behavior of thiol–ene hydrogels by manipulating the degree of network cross-linking and cross-linking peptide sequences. By altering thiol–ene hydrogel protease sensitivity, the mode of thiol–ene hydrogels degradation could be switched between surface erosion and bulk degradation. These studies provide further understanding on the network properties of the thiol–ene hydrogels, which should benefit the utilization of this diverse hydrogel system in tissue engineering applications.

AUTHOR INFORMATION

Corresponding Author

*E-mail: lincc@iupui.edu. Phone: 317-274-0760. Fax: 317-278-2455.

Notes

The authors declare no competing financial interest.

ACKNOWLEDGMENTS

This project was funded by the Department of Biomedical Engineering at IUPUI, a Research Support Funds Grant (RSFG) from IUPUI Office of the Vice Chancellor for Research (OVCR) and NIH/NIBIB (R21EB013717). The authors thank Mr. Asad Raza for his assistance on PEG4NB synthesis.

REFERENCES

(1) Anseth, K. S.; Metters, A. T.; Bryant, S. J.; Martens, P. J.; Elisseeff, J. H.; Bowman, C. N. *J. Controlled Release* **2002**, *78*, 199–209.
(2) Bryant, S. J.; Anseth, K. S. *J. Biomed. Mater. Res.* **2002**, *59*, 63–72.
(3) Peppas, N. A.; Hilt, J. Z.; Khademhosseini, A.; Langer, R. *Adv. Mater.* **2006**, *18*, 1345–1360.
(4) Lin, C. C.; Anseth, K. S. *Pharm. Res.* **2009**, *26*, 631–643.
(5) Metters, A. T.; Anseth, K. S.; Bowman, C. N. *Polymer* **2000**, *41*, 3993–4004.
(6) Metters, A. T.; Bowman, C. N.; Anseth, K. S. *J. Phys. Chem. B* **2000**, *104*, 7043–7049.
(7) Metters, A. T.; Anseth, K. S.; Bowman, C. N. *J. Phys. Chem. B* **2001**, *105*, 8069–8076.
(8) Sawhney, A. S.; Pathak, C. P.; Hubbell, J. A. *Macromolecules* **1993**, *26*, 581–587.
(9) He, S.; Timmer, M. D.; Yaszemski, M. J.; Yasko, A. W.; Engel, P. S.; Mikos, A. G. *Polymer* **2001**, *42*, 1251–1260.
(10) Cho, E.; Kutty, J. K.; Datar, K.; Lee, J. S.; Vyavahare, N. R.; Webb, K. *J. Biomed. Mater. Res., Part A* **2009**, *90A*, 1073–1082.
(11) Elbert, D. L.; Pratt, A. B.; Lutolf, M. P.; Halstenberg, S.; Hubbell, J. A. *J. Controlled Release* **2001**, *76*, 11–25.
(12) Lutolf, M. P.; Lauer-Fields, J. L.; Schmoekel, H. G.; Metters, A. T.; Weber, F. E.; Fields, G. B.; Hubbell, J. A. *Proc. Natl. Acad. Sci. U.S.A.* **2003**, *100*, 5413–5418.
(13) Metters, A.; Hubbell, J. *Biomacromolecules* **2005**, *6*, 290–301.
(14) van de Wetering, P.; Metters, A. T.; Schoenmakers, R. G.; Hubbell, J. A. *J. Controlled Release* **2005**, *102*, 619–627.
(15) Rydholm, A. E.; Bowman, C. N.; Anseth, K. S. *Biomaterials* **2005**, *26*, 4495–4506.
(16) Rydholm, A. E.; Reddy, S. K.; Anseth, K. S.; Bowman, C. N. *Biomacromolecules* **2006**, *7*, 2827–2836.
(17) Rydholm, A. E.; Anseth, K. S.; Bowman, C. N. *Acta Biomater.* **2007**, *3*, 449–455.
(18) Rydholm, A. E.; Reddy, S. K.; Anseth, K. S.; Bowman, C. N. *Polymer* **2007**, *48*, 4589–4600.
(19) Zustiak, S. P.; Leach, J. B. *Biomacromolecules* **2010**, *11*, 1348–1357.
(20) Zustiak, S. P.; Leach, J. B. *Biotechnol. Bioeng.* **2011**, *108*, 197–206.
(21) Lin-Gibson, S.; Jones, R. L.; Washburn, N. R.; Horkay, F. *Macromolecules* **2005**, *38*, 2897–2902.
(22) Fairbanks, B. D.; Schwartz, M. P.; Halevi, A. E.; Nuttelman, C. R.; Bowman, C. N.; Anseth, K. S. *Adv. Mater.* **2009**, *21*, 5005–5010.
(23) Hoyle, C. E.; Bowman, C. N. *Angew. Chem., Int. Ed.* **2010**, *49*, 1540–1573.
(24) Lin, C. C.; Raza, A.; Shih, H. *Biomaterials* **2011**, *32*, 9685–9695.
(25) Fairbanks, B. D.; Singh, S. P.; Bowman, C. N.; Anseth, K. S. *Macromolecules* **2011**, *44*, 2444–2450.
(26) Anderson, S. B.; Lin, C. C.; Kuntzler, D. V.; Anseth, K. S. *Biomaterials* **2011**, *32*, 3564–3574.
(27) Schwartz, M. P.; Fairbanks, B. D.; Rogers, R. E.; Rangarajan, R.; Zaman, M. H.; Anseth, K. S. *Int. Biol.* **2010**, *2*, 32–40.

(28) Benton, J. A.; Fairbanks, B. D.; Anseth, K. S. *Biomaterials* **2009**, *30*, 6593−6603.
(29) Aimetti, A. A.; Machen, A. J.; Anseth, K. S. *Biomaterials* **2009**, *30*, 6048−6054.
(30) DuBose, J. W.; Cutshall, C.; Metters, A. T. *J. Biomed. Mater. Res., Part A* **2005**, *74A*, 104−116.
(31) Lin, C. C.; Metters, A. T. *Pharm. Res.* **2006**, *23*, 614−622.
(32) Fairbanks, B. D.; Schwartz, M. P.; Bowman, C. N.; Anseth, K. S. *Biomaterials* **2009**, *30*, 6702−6707.
(33) Flory, P., *Principles in Polymer Chemistry*; Cornell University Press: Ithaca, NY, 1953.
(34) Lin, C. C.; Metters, A. T. *Adv. Drug Delivery Rev.* **2006**, *58*, 1379−1408.
(35) Anseth, K. S.; Bowman, C. N.; Peppas, N. A. *J. Polym. Sci., Part A: Polym. Chem.* **1994**, *32*, 139−147.
(36) Anseth, K. S.; Bowman, C. N.; BrannonPeppas, L. *Biomaterials* **1996**, *17*, 1647−1657.
(37) Kloxin, A. M.; Benton, J. A.; Anseth, K. S. *Biomaterials* **2010**, *31*, 1−8.
(38) Kloxin, A. M.; Kloxin, C. J.; Bowman, C. N.; Anseth, K. S. *Adv. Mater.* **2010**, *22*, 3484−3494.
(39) Napoli, A.; Valentini, M.; Tirelli, N.; Muller, M.; Hubbell, J. A. *Nat. Mater.* **2004**, *3*, 183−189.
(40) Kraehenbuehl, T. P.; Ferreira, L. S.; Zammaretti, P.; Hubbell, J. A.; Langer, R. *Biomaterials* **2009**, *30*, 4318−4324.
(41) Kraehenbuehl, T. P.; Zammaretti, P.; Van der Vlies, A. J.; Schoenmakers, R. G.; Lutolf, M. P.; Jaconi, M. E.; Hubbell, J. A. *Biomaterials* **2008**, *29*, 2757−2766.
(42) Miller, J. S.; Shen, C. J.; Legant, W. R.; Baranski, J. D.; Blakely, B. L.; Chen, C. S. *Biomaterials* **2010**, *31*, 3736−3743.
(43) Patterson, J.; Hubbell, J. A. *Biomaterials* **2010**, *31*, 7836−7845.
(44) Tsurkan, M. V.; Chwalek, K.; Levental, K. R.; Freudenberg, U.; Werner, C. *Macromol. Rapid Commun.* **2010**, *31*, 1529−1533.